

1  
2  
3  
4  
5  
6  
7

Received Date : 01-Jun-2016

Revised Date : 01-Jul-2016

Accepted Date : 10-Jul-2016

Article type : Regular Paper

**4D *in vivo* imaging of glomerular barrier function in a zebrafish podocyte injury model**

Florian Siegerist<sup>1</sup>, Weibin Zhou<sup>2</sup>, Karlhans Endlich<sup>1</sup>, Nicole Endlich<sup>1\*</sup>

<sup>1</sup>*Department of Anatomy and Cell Biology, University Medicine Greifswald, Greifswald, Germany*

<sup>2</sup>*Department of Pediatrics and Communicable Diseases, University of Michigan, Ann Arbor, Michigan, USA*

\* Address correspondence to Nicole Endlich:

Friedrich-Loefflerstr. 23c, 17487 Greifswald, Germany

Tel: +49 (0) 3834/865303, Fax: +49 (0) 3834/865302,

E-mail: [nicole.endlich@uni-greifswald.de](mailto:nicole.endlich@uni-greifswald.de)

This is the author manuscript accepted for publication and has undergone full peer review but has not been through the copyediting, typesetting, pagination and proofreading process, which may lead to differences between this version and the [Version of Record](#). Please cite this article as doi: [10.1111/apha.12754](https://doi.org/10.1111/apha.12754)

This article is protected by copyright. All rights reserved

Short title: 4D imaging of glomerular filtration

## **Abstract:**

**Aim:** Zebrafish larvae with their simplified pronephros are an ideal model to study glomerular physiology. Although several groups use zebrafish larvae to assess glomerular barrier function, temporary or slight changes are still difficult to measure. Aim of this study was to investigate the potential of *in vivo* two-photon microscopy (2-PM) for long-term imaging of glomerular barrier function in zebrafish larvae.

**Methods:** As a proof of principle we adapted the nitroreductase/metronidazole model of targeted podocyte ablation for 2-PM. Combination with a strain which expresses eGFP-vitamin D-binding protein in the blood plasma led to a strain that allowed induction of podocyte injury with parallel assessment of glomerular barrier function. We used four-dimensional (4D) 2-PM to assess eGFP fluorescence over 26 h in the vasculature and in tubules of multiple zebrafish larvae (5 days post fertilization) simultaneously.

**Results:** By 4D 2-PM we observed that, under physiological conditions, eGFP fluorescence was retained in the vasculature and rarely detected in proximal tubule cells. Application of metronidazole induced podocyte injury and cell-death as shown by TUNEL staining. Induction of podocyte injury resulted in a dramatic decrease of eGFP fluorescence in the vasculature over time (about 50% and 90% after 2 and 12 h, respectively). Loss of vascular eGFP fluorescence was paralleled by an endocytosis-mediated accumulation of eGFP fluorescence in proximal tubule cells, indicating proteinuria.

**Conclusion:** We established a microscopy-based method to monitor the dynamics of glomerular barrier function during induction of podocyte injury in multiple zebrafish larvae simultaneously over 26 h.

**Keywords:** Glomerular filtration, podocyte injury, proteinuria, proximal tubule

This article is protected by copyright. All rights reserved

## Introduction

The glomerular filtration barrier of the kidney is composed of three components: the fenestrated endothelial cells, the glomerular basement membrane (GBM), and the podocytes with a slit diaphragm. Podocytes are highly specialized cells with a complex 3D morphology which is responsible for proper blood filtration in the kidney. These cells cover the outer aspect of the glomerular capillaries by their highly branched cell extensions, the foot processes, and interdigitate in a zipper-like fashion with a slit diaphragm in between (Pavenstädt *et al.* 2003). Impairment of the filtration barrier leads to disruption of the size selectivity and proteinuria, a clinical hallmark of chronic kidney disease. To understand pathogenesis and to screen for potential therapies in animal models which mimic human kidney diseases, quantification of glomerular filtration and proteinuria is undoubtedly important.

The pronephros, the first filtering kidney in developing zebrafish, is an ideal model to study kidney function with a similar glomerular morphology to that of mammals (Drummond & Davidson 2010). It consists of a single glomerulus connected to a pair of tubules which starts filtration at 2 days past fertilization (dpf) and develops a fully working filtration barrier at 3.5 dpf (Drummond 2005; Drummond & Davidson 2010; Kramer-Zucker *et al.* 2005).

Several groups used the zebrafish as a model to study defects of the glomerular filtration barrier (Hanke *et al.* 2015; Hentschel *et al.* 2007; Kotb *et al.* 2014; Rider *et al.* 2012; Wan *et al.* 2015). Currently there are two methods to investigate proteinuria in zebrafish. The first one is to compare intravascular fluorescence intensities of either dextran-injected or transgenic zebrafish larvae by fluorescence microscopy. The second approach is to check for tubular endocytosis in histological sections subsequent to intravenous injection of fluorescently labeled 10 and 500 kDa dextrans. A disadvantage of both methods is that temporary changes in glomerular barrier function are difficult to measure. Until today there is no existing method for continuous monitoring of glomerular barrier function in zebrafish larvae over hours or days.

While earlier studies required labor-intensive intravenous injection of fluorescence-labeled molecules like inulin or dextran for assessment of glomerular filtration recently a new transgenic zebrafish strain was established which endogenously

expresses eGFP-labeled vitamin D-binding protein (eGFP-DBP) (Ashworth *et al.* 2010; Kotb *et al.* 2014; Rider *et al.* 2012; Xie *et al.* 2010). EGFP-DBP (78 kDa), a protein of the albumin family, is synthesized in the liver under control of the liver-type fatty acid binding protein (*l-fabp*) promoter and secreted into the blood plasma. Under physiological conditions eGFP-DBP is retained in the vasculature due to the size selectivity of the glomerular filtration barrier. After impairment of the filtration barrier, a decrease of the intravascular eGFP-DBP and megalin-mediated endocytosis of eGFP-DBP in proximal tubule cells (PTCs) were described (Ashworth *et al.* 2010; Kotb *et al.* 2014; Kotb *et al.* 2016; Wan *et al.* 2015).

Due to the availability of transparent and fluorophore-expressing strains, zebrafish larvae are a powerful model for microscopy-based *in vivo* analysis of the glomerular filtration barrier, especially by long-term two photon microscopy (2-PM) (Endlich *et al.* 2014; Kotb *et al.* 2016). To study the development and dynamics of proteinuria in zebrafish larvae *in vivo*, we used the nitroreductase (NTR)/metronidazole (MTZ) model of targeted podocyte ablation. This zebrafish strain expresses the E.coli-derived enzyme NTR under the control of the podocyte-specific podocin (*nphs2*) promoter. After application of the prodrug MTZ to the medium of the larvae, podocytes become injured, apoptotic and detach (Huang *et al.* 2013; Zhou & Hildebrandt 2012). In the present study, we utilized different zebrafish strains to generate a new transgenic zebrafish strain that enables long-term *in vivo* 2-PM imaging to induce and track changes of glomerular barrier function over up to 26 h.

## Material and Methods

### Zebrafish stocks

Zebrafish stocks and larvae were maintained as described previously (Kotb *et al.* 2014; Müller *et al.* 2011). The *Cade* strain (Tg(*l-fabp*:eGFP-DBP; *mitfa*<sup>w2/w2</sup>; *roy*<sup>a9/a9</sup>) expresses the 78 kDa eGFP-vitamin D binding-protein in the transparent *Casper* background (Kotb *et al.* 2014; Xie *et al.* 2010). The Tg(*nphs2*:Eco.NfsB-mCherry) strain (Zhou & Hildebrandt 2012) was cross-bred with *Casper* (*mitfa*<sup>w2/w2</sup>; *roy*<sup>a9/a9</sup>) (White *et al.* 2008) resulting in a new strain named *Nury* (Tg(*nphs2*:Eco.NfsB-mCherry); *mitfa*<sup>w2/w2</sup>; *roy*<sup>a9/a9</sup>). For evaluation of the glomerular barrier function *Nury* was cross-bred with *Cade* resulting in a new transparent strain with eGFP-DBP in the blood plasma and NTR-mCherry in podocytes (Tg(*l-fabp*:eGFP-DBP;

Tg(*nphs2*:Eco.NfsB-mCherry) *mitfa*<sup>w2/w2</sup>; *roy*<sup>a9/a9</sup>). This strain was named *BlooP* for **blood** and **podocytes**. All experiments were performed in accordance with German law and were overseen by the agencies of the Federal State of Mecklenburg-Western Pomerania. All 2-PM experiments were performed at 22°C. Metronidazole (Sigma-Aldrich, St.Louis, MO, USA) was freshly prepared in 0.1% DMSO-E3. Zebrafish larvae were treated at 3 and 5 dpf with 1 or 5 mM MTZ.

## Histology

Cryosections and confocal microscopy were performed as described elsewhere (Endlich *et al.* 2014). TUNEL assay (in situ Cell Death Detection Kit, Fluorescein, Roche, Basel, Switzerland) was prepared according to the manufacturer's description followed by 0.013 mg/ml Hoechst 33342 (Sigma-Aldrich, St.Louis, MO, USA) and mounting in Mowiol (Carl Roth, Karlsruhe, Germany).

## Imaging

For *in vivo* imaging up to ten larvae at 5 dpf were embedded as described before (Endlich *et al.* 2014). After hardening, the larvae were covered with 1 mM MTZ in 0.1% DMSO in E3 medium containing 0.1% tricaine. 2-PM was performed with a LSM710MP (Carl Zeiss Microimaging, Jena, Germany) and 20x (1.0 NA) water immersion objective with a pulsed Ti-Sapphire laser (Chamaeleon, Coherent, Santa Clara, CA, USA). Every 30 minutes automated z-stacks of each larva over 118 µm were recorded. Fluorescence measurements and 3D reconstruction was performed with Zeiss ZEN 2010 software (Carl Zeiss Microimaging, Jena, Germany) and arranged to 4D movies with ImageJ (NIH, USA). Statistics (Student's t-test) were calculated with Excel (Version 14.0.7, Microsoft, Redmond, WA, USA).

## Results

### Application of MTZ to *Nury* larvae promotes apoptosis in podocytes

We crossed the Tg(*nphs2*:Eco.NfsB-mCherry) zebrafish strain which expresses the prokaryotic enzyme NTR and mCherry under the control of the podocyte-specific *podocin* promoter (Zhou & Hildebrandt 2012) with the transparent zebrafish *Casper* (*mitfa*<sup>w2/w2</sup>; *roy*<sup>a9/a9</sup>) (White *et al.* 2008; Zhou & Hildebrandt 2012). In order to induce proteinuria, larvae (3 dpf) of the new strain (*Nury* - **Nitroreductase-mCherry**) were incubated for 20 h with 5 mM MTZ. To verify MTZ-induced apoptosis in *Nury* larvae,

sections were stained by terminal deoxynucleotidyl transferase dUTP nick end labeling (TUNEL). In contrast to DMSO (0.1%) treated larvae (control), a widespread TUNEL signal was detected (Fig. 1a), which co-localized with podocytes and Hoechst labeled nuclei (Fig.1b) indicating specific cell death of podocytes.

### **Live assessment of glomerular barrier function during podocyte injury**

For further assessment of the glomerular barrier function, we established a new zebrafish strain (*BlooP*) on the transparent *Casper* background which additionally expresses the 78 kDa eGFP-labeled Vitamin D-binding protein (eGFP-DBP) under control of the *liver-type fatty acid binding protein* promoter in the blood plasma.

To verify expression of NTR-mCherry at 5 dpf we performed 2-PM two-channel scans for mCherry and eGFP (Fig. 2a). The following scans captured eGFP fluorescence alone to minimize bleaching effects by the significantly shorter excitation wavelength of mCherry (Fig. 2b-f). In order to induce proteinuria 1 mM MTZ was added to the medium of *BlooP* larvae at  $t = 0$ . MTZ treatment led to a significant decrease of relative eGFP fluorescence intensity in the dorsal aorta of *BlooP* ( $n = 33$ ) as compared to *Cade* control larvae ( $n = 28$ ). At  $t = 24$  h a decrease to 0.6% was measured ( $p < 0.001$ , Student's t-test, Fig. 2g).

Additionally, a significant increase of the eGFP fluorescence in PTCs was detected beginning at  $t = 12$  h due to an endocytic uptake of eGFP-DBP which passed the leaky filtration barrier after podocyte injury (Fig. 2c-f; movie 1). This increase was found in 89% (SD = 13.9%,  $p = 0.0002$ ) of *BlooP* larvae ( $n = 33$ ) compared to 6.7% (SD = 4.6%) of control larvae ( $n = 28$ ) in three individual experiments (Fig. 2h).

While Figure 2i shows an intensive eGFP signal in PTCs (typical position of PTCs is marked by yellow circles) in a cross section of a *BlooP* larva (6 dpf) after 2-PM, PTCs of the shown *Cade* control larva shows no accumulation of eGFP-DBP. However only larvae (*BlooP* or *Cade*) showing eGFP-DBP accumulation in 2-PM showed eGFP-positive PTCs in confocal microscopy of cryosections (in  $n = 3$  individual experiments).

### **4D *in vivo* imaging of proteinuria**

Movie 2 offers a unique 4D view on the particular changes following podocyte injury. At  $t = 0$ , the glomerular tuft is visible ventral to the dorsal aorta (Fig. 3 arrows). EGFP

appears between  $t = 12$  h and  $t = 13$  h in PTCs and unveils its contorted 3D structure. Over the whole period of MTZ treatment the intravascular fluorescence intensity of *BlooP* larvae decreases due to the loss of eGFP-DBP from the blood as shown in movie 3. In contrast to that, the intravascular fluorescence intensity of *Cade* larvae increases over the imaging period.

## Discussion

Here we demonstrate that the zebrafish larva is an ideal model to study the glomerular filtration barrier and the development of proteinuria *in vivo*.

For the last decades the most popular model organisms in renal research have been rodents. Despite of their many advantages, mice and rats lack easy accessibility of glomeruli and only strains with superficial glomeruli, like Munich-Wistar rats are suitable for *in vivo* imaging (Russo *et al.* 2007; Schießl *et al.* 2016). Additionally, most *in vivo* multiphoton-imaging approaches in mammals require rather complex and time consuming preparations until filtering glomeruli can be visualized (Brahler *et al.* 2016; Peti-Peterdi & Sipos 2010; Schießl *et al.* 2016) or appear to be rather artificial (Kistler *et al.* 2014). In contrast to that, our model has no limitations in accessibility of glomeruli and can be applied to all available zebrafish strains, mutants and especially gene knockdown strategies for evaluation of specific protein function e.g. with morpholinos. Moreover, due to semi-automated simultaneous imaging of a group of larvae, our technique offers the opportunity for an increased throughput analysis of differently treated zebrafish larvae to evaluate the potential of particular treatments prior to labor- and cost-intensive experiments in a higher vertebrate model.

Although there are broad similarities between the larval zebrafish and mammalian glomerular filtration, there are also important differences. Compared to mammals the arterial blood pressure reaches a relatively low maximum systolic pressure of about 0.5 mmHg at 4 dpf (Pelster & Burggren 1996). Additionally, the major part of tubular flow in larval zebrafish is dependent on the function of motile cilia in the pronephros (Kramer-Zucker *et al.* 2005). Like most teleost species, zebrafish lack the albumin gene but possess another similar protein of the albumin family, the vitamin-D binding protein gene (*dbp*) (Noel *et al.* 2010) which was labeled by eGFP in the *Cade* strain. Since both proteins have a similar size (66 kDa albumin versus 78 kDa eGFP-DBP),

it is possible to study the glomerular barrier function in real time with this transgenic strain.

Compared to BlooP larvae treated with 1 mM MTZ, the control larvae (*Cade*) showed increasing expression of eGFP-DBP as seen by eGFP fluorescence in the vasculature during the imaging period between 5 and 6 dpf. These findings are consistent with previous investigations that showed increasing activity of the *l-fabp* promoter between 4 to 7 dpf in larval zebrafish (Her *et al.* 2003; Her *et al.* 2004).

In this study, we underline the important role of podocytes for the integrity of the intact glomerular filtration barrier. In contrast to Russo and coworkers who postulated that the filtration barrier leaks protein, especially albumin, at nephrotic levels which is salvaged by PTCs, (Russo *et al.* 2007) we only observed accumulation of eGFP-DBP in PTCs under healthy conditions in 6.7% of *Cade* control larvae, indicating that loss of eGFP-DBP from the vasculature of healthy zebrafish larvae is a rather rare event. However, after impairment of the filtration barrier through MTZ induced podocyte injury, (Pisharath *et al.* 2007; Zhou & Hildebrandt 2012) we found a rapid increase of endocytic uptake of filtered eGFP-DBP in PTCs.

Previous studies which investigated glomerular filtration with eGFP-labeled DBP in zebrafish focused on the measurement of fluorescence intensity in the eye (Hanke *et al.* 2015) or in the vasculature (Kotb *et al.* 2014). Another approach is to measure levels of filtered eGFP-DBP in the medium of a group of zebrafish larvae by dot blot or by ELISA analysis for eGFP (Hanke *et al.* 2015; Zhou & Hildebrandt 2012). A disadvantage of the two latter methods is that temporary and intermittent alterations of the glomerular filtration barrier are hardly detectable. We have overcome this disadvantage by continuous measurement of eGFP fluorescence over 26 h so that even temporary changes of the eGFP-DBP fluorescence are detectable. Faster (within minutes) alterations of the intravascular fluorescence intensity can also be tracked with our technique, simply by using a shorter recording interval.

Taken together, this animal model of the glomerular filtration barrier allows us to follow the development and dynamics of proteinuria in 4D in a group of larvae over extended time periods of 26 h *in vivo*.

## Acknowledgments



The excellent technical assistance of Oliver Zabel is greatly acknowledged. This study was supported by a grant of the European Union within the 7th framework program to K.E. (project "EnVision", grant agreement no. 264143), by grants of the German Federal Ministry of Education and Research (BMBF) to N.E. (project "STOP-FSGS", grant no. 01GM1518B) and was supported by a scholarship of the Gerhard Domagk program of the University Medicine Greifswald to F.S.

## Conflicts of interest

None.

## References

- Ashworth, S., Teng, B., Kaufeld, J., Miller, E., Tossidou, I., Englert, C., Bollig, F., Staggs, L., Roberts, I.S.D., Park, J.-K., Haller, H. & Schiffer, M. 2010. Cofilin-1 inactivation leads to proteinuria--studies in zebrafish, mice and humans. *PLoS one* **5**, e12626.
- Brahler, S., Yu, H., Suleiman, H., Krishnan, G.M., Saunders, B.T., Kopp, J.B., Miner, J.H., Zinselmeyer, B.H. & Shaw, A.S. 2016. Intravital and Kidney Slice Imaging of Podocyte Membrane Dynamics. *Journal of the American Society of Nephrology*.
- Drummond, I.A. 2005. Kidney development and disease in the zebrafish. *Journal of the American Society of Nephrology : JASN* **16**, 299–304.
- Drummond, I.A. & Davidson, A.J. 2010. Zebrafish kidney development. *Methods in cell biology* **100**, 233–260.
- Endlich, N., Simon, O., Göpferich, A., Wegner, H., Moeller, M.J., Rumpel, E., Kotb, A.M. & Endlich, K. 2014. Two-photon microscopy reveals stationary podocytes in living zebrafish larvae. *Journal of the American Society of Nephrology : JASN* **25**, 681–686.
- Hanke, N., King, B.L., Vaske, B., Haller, H. & Schiffer, M. 2015. A Fluorescence-Based Assay for Proteinuria Screening in Larval Zebrafish (*Danio rerio*). *Zebrafish* **12**, 372–376.
- Hentschel, D.M., Mengel, M., Boehme, L., Liebsch, F., Albertin, C., Bonventre, J.V., Haller, H. & Schiffer, M. 2007. Rapid screening of glomerular slit diaphragm integrity in larval zebrafish. *AJP: Renal Physiology* **293**, F1746-F1750.

- Her, G.M., Chiang, C.C., Chen, W.Y. & Wu, J.L. 2003. In vivo studies of liver-type fatty acid binding protein (L-FABP) gene expression in liver of transgenic zebrafish (*Danio rerio*). *FEBS letters* **538**, 125–133.
- Her, G.M., Chiang, C.C. & Wu, J.L. 2004. Zebrafish intestinal fatty acid binding protein (I-FABP) gene promoter drives gut-specific expression in stable transgenic fish. *Genesis (New York, N. Y. : 2000)* **38**, 26–31.
- Huang, J., McKee, M., Huang, H.D., Xiang, A., Davidson, A.J. & Lu, H.A.J. 2013. A zebrafish model of conditional targeted podocyte ablation and regeneration. *Kidney Int* **83**, 1193–1200.
- Kistler, A.D., Caicedo, A., Abdulreda, M.H., Faul, C., Kerjaschki, D., Berggren, P.O., Reiser, J. & Fornoni, A. 2014. In vivo imaging of kidney glomeruli transplanted into the anterior chamber of the mouse eye. *Scientific reports* **4**, 3872.
- Kotb, A.M., Müller, T., Xie, J., Anand-Apte, B., Endlich, K. & Endlich, N. 2014. Simultaneous assessment of glomerular filtration and barrier function in live zebrafish. *American journal of physiology. Renal physiology* **307**, 34.
- Kotb, A.M., Simon, O., Blumenthal, A., Vogelgesang, S., Dombrowski, F., Amann, K., Zimmermann, U., Endlich, K. & Endlich, N. 2016. Knockdown of ApoL1 in Zebrafish Larvae Affects the Glomerular Filtration Barrier and the Expression of Nephin. *PloS one* **11**, e0153768.
- Kramer-Zucker, A.G., Wiessner, S., Jensen, A.M. & Drummond, I.A. 2005. Organization of the pronephric filtration apparatus in zebrafish requires Nephin, Podocin and the FERM domain protein Mosaic eyes. *Developmental biology* **285**, 316–329.
- Müller, T., Rumpel, E., Hradetzky, S., Bollig, F., Wegner, H., Blumenthal, A., Greinacher, A., Endlich, K. & Endlich, N. 2011. Non-muscle myosin IIA is required for the development of the zebrafish glomerulus. *Kidney international* **80**, 1055–1063.
- Noel, E.S., Reis, M.D., Arain, Z. & Ober, E.A. 2010. Analysis of the Albumin/alpha-Fetoprotein/Afamin/Group specific component gene family in the context of zebrafish liver differentiation. *Gene expression patterns : GEP* **10**, 237–243.
- Pavenstädt, H., Kriz, W. & Kretzler, M. 2003. Cell biology of the glomerular podocyte. *Physiological reviews* **83**, 253–307.

- Pelster, B. & Burggren, W.W. 1996. Disruption of hemoglobin oxygen transport does not impact oxygen-dependent physiological processes in developing embryos of zebra fish (*Danio rerio*). *Circulation research* **79**, 358–362.
- Peti-Peterdi, J. & Sipos, A. 2010. A high-powered view of the filtration barrier. *Journal of the American Society of Nephrology : JASN* **21**, 1835–1841.
- Pisharath, H., Rhee, J.M., Swanson, M.A., Leach, S.D. & Parsons, M.J. 2007. Targeted ablation of beta cells in the embryonic zebrafish pancreas using *E. coli* nitroreductase. *Mechanisms of development* **124**, 218–229.
- Rider, S.A., Tucker, C.S., del-Pozo, J., Rose, K.N., MacRae, C.A., Bailey, M.A. & Mullins, J.J. 2012. Techniques for the in vivo assessment of cardio-renal function in zebrafish (*Danio rerio*) larvae. *The Journal of physiology* **590**, 1803–1809.
- Russo, L.M., Sandoval, R.M., McKee, M., Osicka, T.M., Collins, A.B., Brown, D., Molitoris, B.A. & Comper, W.D. 2007. The normal kidney filters nephrotic levels of albumin retrieved by proximal tubule cells. Retrieval is disrupted in nephrotic states. *Kidney international* **71**, 504–513.
- Schießl, I.M., Hammer, A., Kattler, V., Gess, B., Theilig, F., Witzgall, R. & Castrop, H. 2016. Intravital Imaging Reveals Angiotensin II-Induced Transcytosis of Albumin by Podocytes. *Journal of the American Society of Nephrology : JASN* **27**, 731–744.
- Wan, X., Chen, Z., Choi, W.-I., Gee, H.Y., Hildebrandt, F. & Zhou, W. 2015. Loss of Epithelial Membrane Protein 2 Aggravates Podocyte Injury via Upregulation of Caveolin-1. *Journal of the American Society of Nephrology : JASN*.
- White, R.M., Sessa, A., Burke, C., Bowman, T., LeBlanc, J., Ceol, C., Bourque, C., Dovey, M., Goessling, W., Burns, C.E. & Zon, L.I. 2008. Transparent adult zebrafish as a tool for in vivo transplantation analysis. *Cell stem cell* **2**, 183–189.
- Xie, J., Farage, E., Sugimoto, M. & Anand-Apte, B. 2010. A novel transgenic zebrafish model for blood-brain and blood-retinal barrier development. *BMC Dev Biol* **10**, 76.
- Zhou, W. & Hildebrandt, F. 2012. Inducible podocyte injury and proteinuria in transgenic zebrafish. *Journal of the American Society of Nephrology : JASN* **23**, 1039–1047.

### Figure Legends:

**Figure 1:** (a) Positive TUNEL signal in cross sections of *Nury* larvae after 20 h exposition to 5 mM MTZ. In contrast to control larvae, a decrease of mCherry fluorescence of podocytes was found in *Nury* larvae ( $n = 3$  individual experiments, scale bar represents 10  $\mu\text{m}$ ) (b) TUNEL signal co-localized with remaining mCherry fluorescence and nuclear Hoechst staining (scale bar represents 5  $\mu\text{m}$ ).

**Figure 2:** Single frames from z-stacks of a living *BlooP* larva exposed to 1 mM MTZ over 26 h. mCherry and eGFP multitrack scan at  $t = 0:00$  (a). Following eGFP scans up to  $t = 26:00$  h show progressive accumulation of eGFP-DBP in PTCs (arrowheads) and a decrease of fluorescence in vasculature (b-f). Scale bar represents 50  $\mu\text{m}$ . *BlooP* larvae showed a significant higher decrease of the relative eGFP fluorescence intensity compared to control (*Cade*) measured in the dorsal aorta (g). Mean values of  $n = 30$  *BlooP* larvae from three individual experiments compared to  $n = 28$  *Cade* larvae. Error bars indicate standard error mean. [‡]:  $p < 0.001$ . h shows that 89% (SD = 13.9%,  $n = 33$ ) of *BlooP* larvae treated with 1 mM MTZ showed accumulation of eGFP in PTCs compared to 6.7% of control larva (SD = 4.6%,  $n = 28$ ). Only eGFP-DBP accumulation was observed by confocal microscopy of cryosections in larvae that showed appearance of eGFP-DBP in 2-PM (l). The red line in picture l encircles the position of the glomerulus, the yellow line of the proximal tubule. Ventral eGFP signal is due to *I-fabp* expression in hepatocytes (representative images of  $n = 3$  independent experiments; scale bar represents 25  $\mu\text{m}$ ).

**Figure 3:** Single frames of 3D reconstructions of z-stacks of *BlooP* and *Cade* larvae show enhanced spatial discrimination of the progress of proteinuria induced by MTZ treatment while *Cade* control larvae showed increasing intravascular fluorescence

(arrows: glomerular tuft, asterisks: dorsal aorta, arrowheads: PTCs; scale bar represents 50  $\mu\text{m}$ ).

### **Movie 1**

Movie 1 shows 2-PM z-stacks of a *BlooP* larva at 5 dpf at  $t = 1$  h, 7.5 h, 12.5 h, 26 h in 1 mM MTZ.

### **Movie 2**

Movie 2 shows a 4D reconstruction of a *BlooP* larva at 5 dpf over 26 h in 1 mM MTZ. The decrease of eGFP fluorescence in the blood and accumulation of eGFP-DBP in the PTCs can be distinguished over the time.

### **Movie 3**

Movie 3 shows the 4D reconstruction of a *Cade* larva at 5 to 6 dpf and serves as control to movie 2. An increase of the fluorescence intensity in the blood can be seen as well as no accumulation of eGFP in PTCs compared to movie 2.

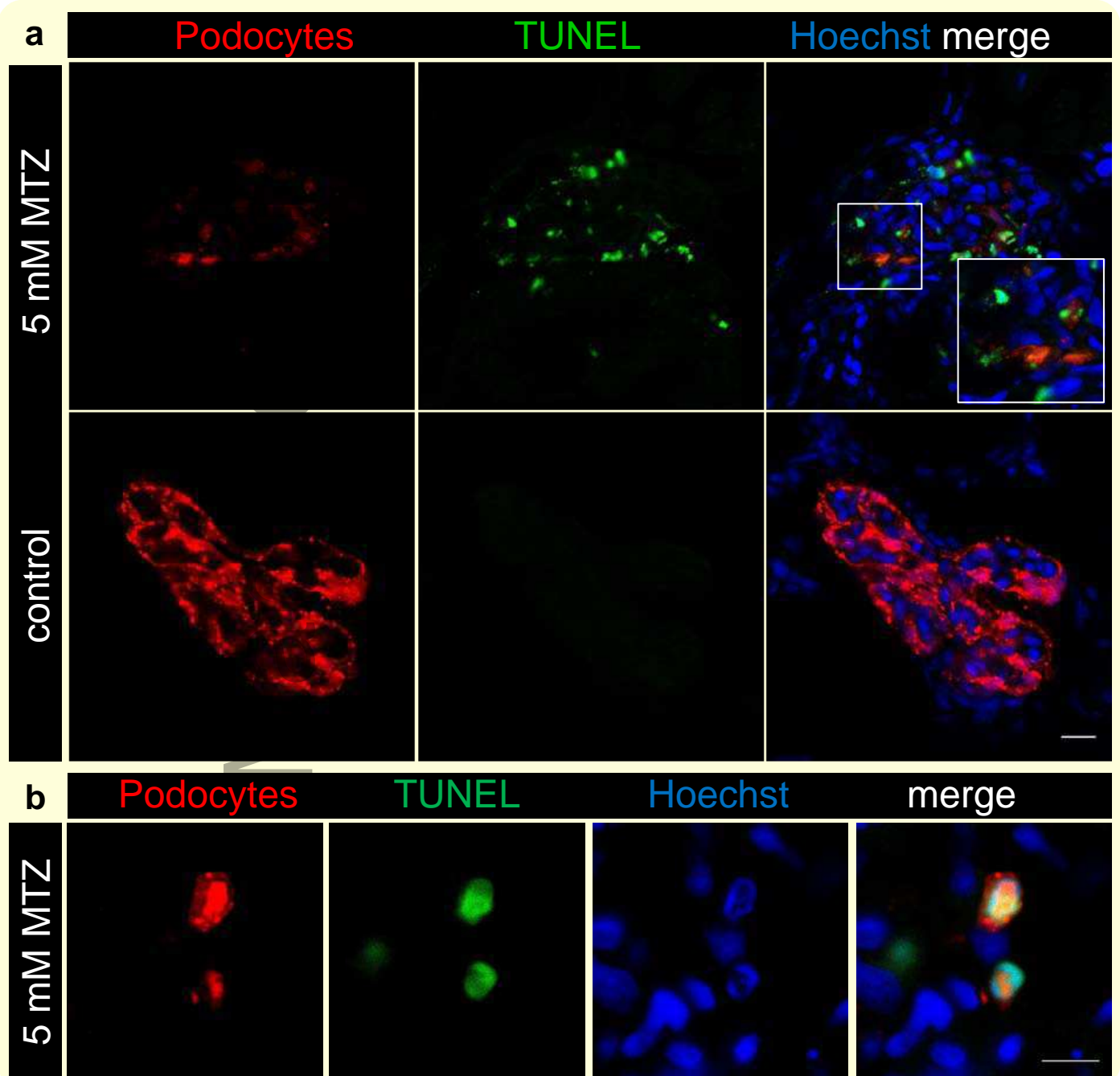
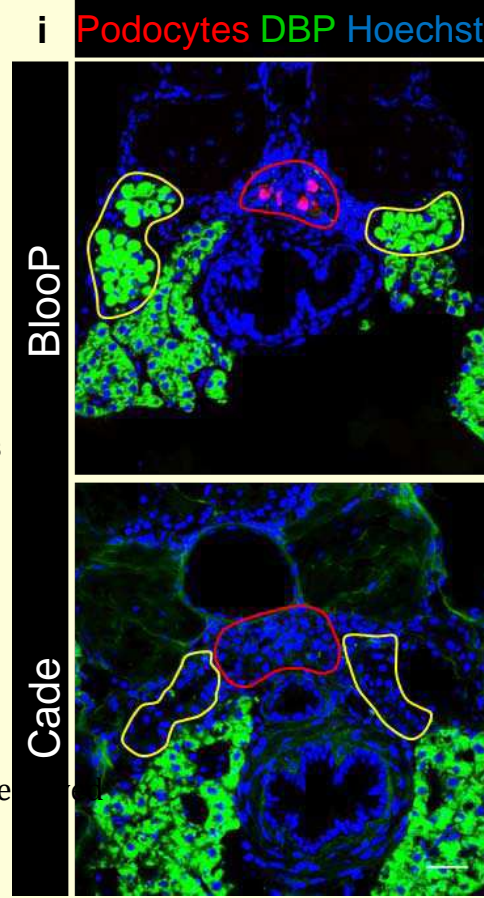
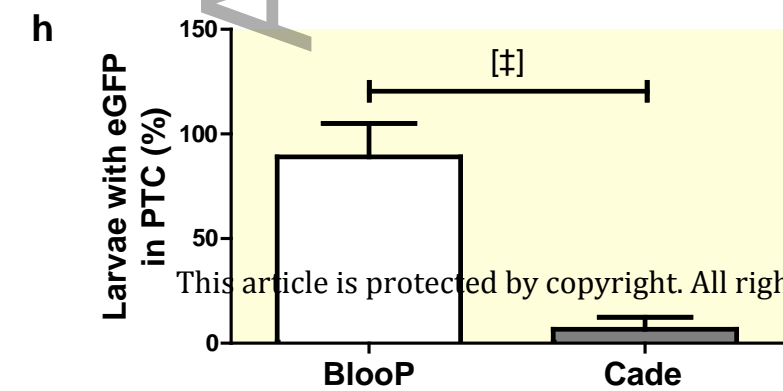
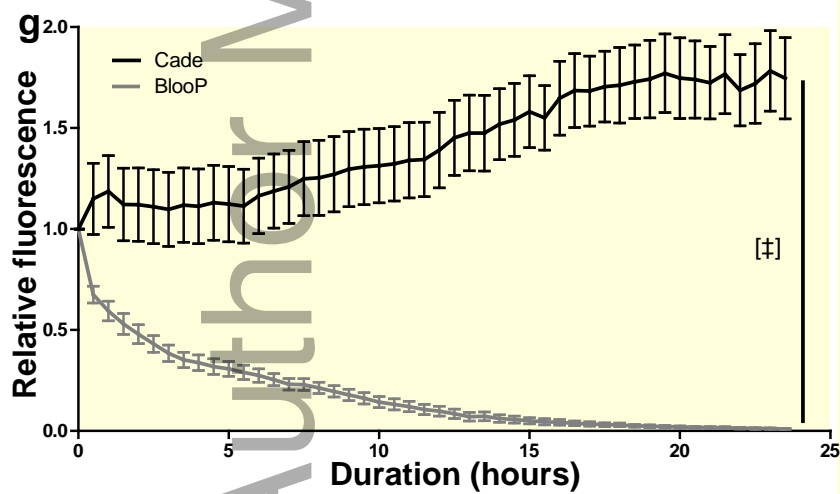
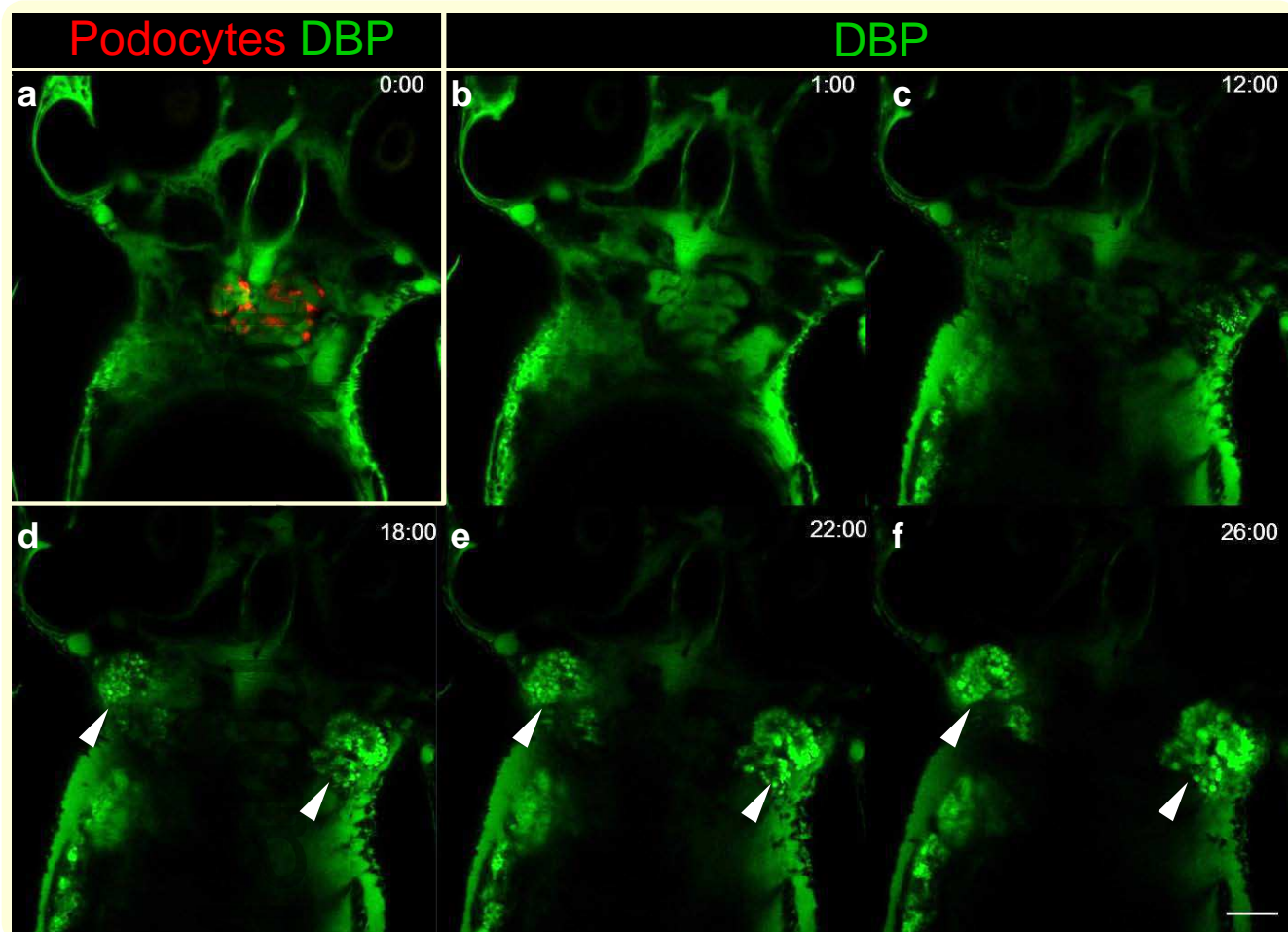
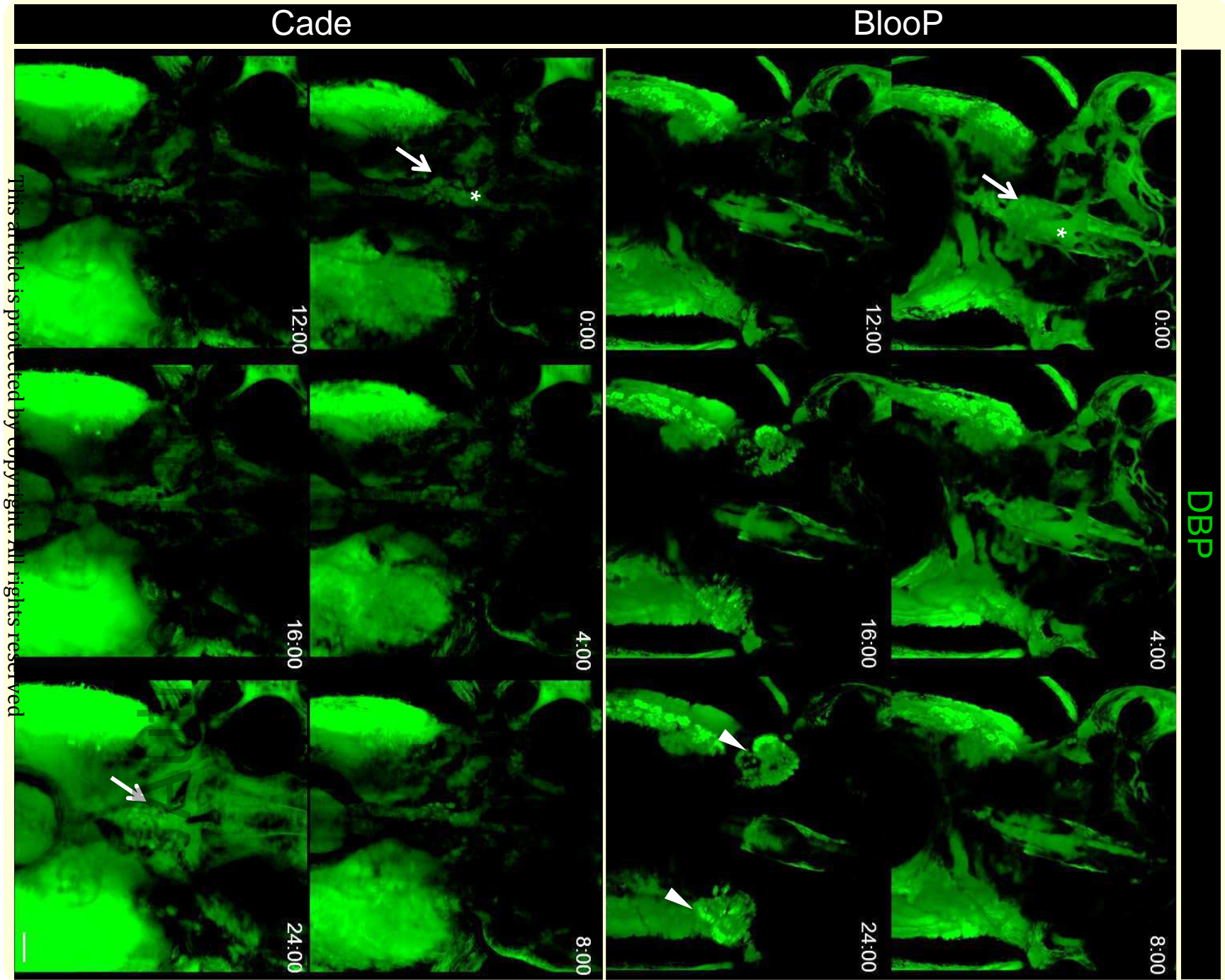


Figure 2





This article is protected by copyright; all rights reserved